ELSEVIER

Journal of Molecular Structure: THEOCHEM 767 (2006) 23–28

THEO CHEM

www.elsevier.com/locate/theochem

Vibrational analysis of the inelastic neutron ascattering spectra of electron donor–acceptor complexes. II. Tetracyanoethylene–perylene by electronic structure calculations

Jennifer A. Ciezak [a,*], Juscelino B. Leão [a], Bruce S. Hudson [b]

[a] *NIST Center for Neutron Research, 100 Bureau Dr. MS 8562, Gaithersburg, MD 20899, USA*
[b] *Department of Chemistry, Syracuse University, Syracuse, NY 13210, USA*

Received 13 March 2006; accepted 12 April 2006
Available online 8 May 2006

Abstract

The vibrational spectra of the electron donor–acceptor complex, tetracyanoethylene–perylene were measured at 4 K by inelastic neutron scattering (INS) using the filter analyzer neutron spectrometer (FANS) and at 20 K using the TOSCA instrument. A direct comparison of the measured spectrum was made to density functional calculations using the B3LYP/6-31G** treatment for the isolated complex, the PW91 pseudopotential plus plane-wave basis and the BLYP/dnd atom-centered basis solid-state methods. In general, comparisons of the observed and simulated spectra revealed that the PW91 method is slightly superior to the B3LYP/6-31G** and BLYP/dnd methods in predicting both vibrational frequency and intensity above 200 cm^{-1}. Below 200 cm^{-1}, the BLYP/dnd calculations gave slightly better intensity agreement. Six intermolecular vibrations were theoretically predicted with the three calculation methods and were experimentally confirmed. In addition, the molecular motions of the vibrations observed in the INS spectrum were tentatively assigned. Our calculations show that solid-state calculations are not required, at least in the case of the TCNE–perylene complex, to obtain reasonably accurate vibrational frequency information of electron donor–acceptor complexes.

Keywords: Inelastic neutron scattering; Electron donor–acceptor complexes; Vibrational spectroscopy

1. Introduction

The intermolecular interactions of electron donor–acceptor (EDA) complexes play a direct role in producing novel electronic, magnetic, and optical functionality [1]. In the crystalline state, the donor and acceptor molecules alternate in a stack-like arrangement and many of the chemical and physical properties of EDA complexes are dependent upon the degree of interaction between the donor and acceptor molecules. The non-covalent bonding arrangement between the two components poses a special challenge in obtaining accurate theoretical descriptions of EDA complexes. Recently, our laboratories described the applicability of solid-state electronic structure calculations to obtain molecular geometries and vibrational information of the EDA complex, tetracyanoethylene–hexamethylbenzene [2]. This work is part of a series that will focus on gaining a deeper understanding of how reliable density functional theory is for several EDA complexes. In this respect, this report will focus on the EDA complex formed between tetracyanoethylene and perylene (TCNE–perylene).

The crystal structure of the TCNE–perylene complex is rather unusual in that the TCNE molecule is positioned over one of the peripheral rings of the perylene molecule, as is shown in Fig. 1 [3]. This arrangement is not the most energetically favorable from the viewpoint of the standard electron donor–acceptor theory put forth by Mulliken [4], but this geometry may have the lowest achievable zero point energy, due to dispersion or repulsive forces in the crystal [3]. Several other EDA complexes with large aromatic rings, such as TCNE–pyrene [5] and TCNE–naphthalene [6] have also been found to have this type of molecular arrangement. A strong interaction between the neighboring columns of TCNE–perylene causes the TCNE nitrile groups to be slightly bent out-of-plane. The structural abnormalities found in the TCNE–perylene complex do not affect the nature of the electron

* Corresponding author. Present address: US Army Research Laboratory, Weapons and Materials Research Directorate, Propulsion Science Branch, Aberdeen Proving Ground, MD 21005, USA. Tel.: +1 301 975 6082; fax: +1 301 921 9847.
E-mail address: jciezak@arl.army.mil (J.A. Ciezak).

0166-1280/$ - see front matter © 2006 Elsevier B.V. All rights reserved.
doi:10.1016/j.theochem.2006.04.037

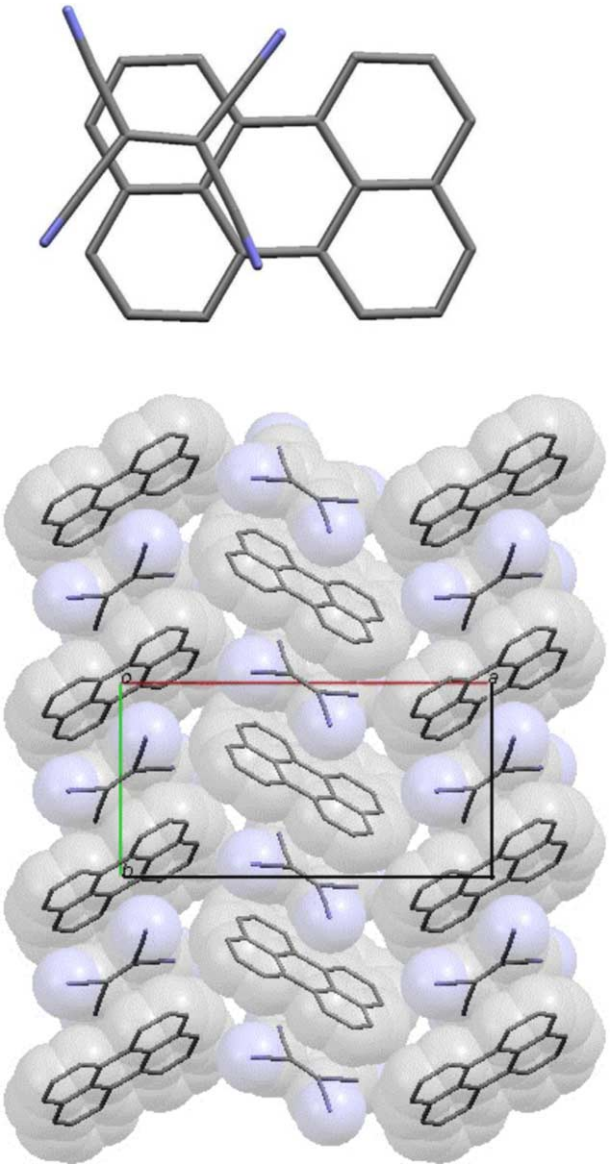

Fig. 1. (a) An isolated complex of the TCNE–perylene complex, shown without hydrogen atoms for clarity. (b) The unit cell of the TCNE–perylene complex, shown without hydrogen atoms for clarity.

donor–acceptor interaction and may be partially responsible for the large third-order optical non-linearity observed for the complex [7].

In order to exploit the macroscopic properties of EDA complexes, a deeper understanding of the fundamental solid-state interactions and dynamics is necessary. This can be accomplished through the use of theoretical models, but in many cases accurate theoretical descriptions are lacking for EDA complexes. By using a combined theoretical/experimental approach, a fundamental test of the theoretical method being used can be performed. Inelastic neutron scattering (INS) is an experimental vibrational spectroscopic technique that is particularly amenable in this regard because of the ease of comparison to theoretical results. Investigations of this type are numerous (see for example, Ref. [2] and Refs. therein, [8–13]). Theoretical inelastic neutron scattering spectra can be directly correlated to the normal mode eigenvectors, which are part of the standard output of quantum mechanical calculations. The vibrational intensities of all lattice and internal modes are observed in direct proportion to the hydrogen displacement for a particular normal mode of vibration. Using this combined theoretical/experimental approach we have tested the applicability of three density functional methods to provide an accurate description of the vibrational dynamics of the TCNE–perylene complex.

2. Materials and methods

The INS spectra were recorded using the filter analyzer neutron spectrometer (FANS) [14] located at the NIST Center for Neutron Research [15] and the time-of-flight spectrometer, TOSCA, located at the ISIS facility of the Rutherford Appleton Facility. Specific details regarding the instrumental configuration of FANS and TOSCA are available in Refs. [14,16–18], respectively. The vibrational frequencies of neat perylene were determined from the inelastic neutron scattering spectrum [19] obtained from the INS database maintained by the ISIS facility.

The EDA complex formed between TCNE and perylene was synthesized according to previously reported methods [3]. Approximately, three grams of sample material was ground into a fine powder and loaded into cryostats held at 4 and 20 K for the duration of the FANS and TOSCA experiments, respectively. The experimental INS spectrum obtained using the FANS instrument was normalized with respect to the background contribution by using the Data Analysis and Visualization Environment (DAVE) [20].

The TCNE–perylene crystal parameters used for the solid-state DFT calculations were obtained from the room temperature crystal structure [3] which is shown in Fig. 1. The room temperature unit cell parameters are as follows: space group $P21/a$, $a=15.763$ Å, $b=8.234$ Å, $c=7.346$ Å, $\beta=96.4°$ and $Z=2$. The solid-state optimized unit cell geometries were obtained using the BLYP functional [21], as implemented in the DMol^3 program [22,23], and the PW91 functional [24] of the VASP program [25]. The BLYP calculations employed a double numeric basis set with polarization functions (dnd) and 'fine' grid spacing. Vanderbilt ultrasoft pseudopotentials and Monkhorst-Pack k-point generation methods were employed in construction of the PW91 calculations [26]. Both the BLYP/dnd and PW91 calculations were optimized until the difference in the electronic energies of subsequent energies was less than 10^{-6} a.u. The PW91 calculations were run at 280, 430, 545 and 645 eV to test for convergence, which was noted at 545 eV. A geometry optimization of an isolated TCNE–perylene unit was performed using the B3LYP [27] density functional with a 6-31G** basis set, as implemented in GAUSSIAN 98 [28]. The Hessian matrices were obtained by calculating the second derivatives of energy analytically for both the PW91 and BLYP/dnd solid-state calculations. The Hessian matrix was found by analytic second derivatives for the B3LYP/6-31G** calculation. The B3LYP/6-31G** vibrational frequencies are scaled uniformly by 0.987 to improve agreement with

experimental values. The BLYP/dnd and PW91 frequencies are unscaled.

Simulated INS spectra were constructed from the quantum chemical output, which included the normal mode eigenvectors, using the aClimax program v. 5.5.0 [29]. The scattering cross-sections of all the atoms in the complex were taken into account in the construction of the simulated spectra. Combinations, overtones, and phonon wings are included to four quanta in all simulated spectra.

3. Results and discussion

The inelastic neutron scattering vibrational frequencies of the TCNE–perylene complex and neat perylene are presented in Table 1. The results of both the TOSCA and FANS experiments are presented as well as a brief description of the molecular motions associated with these vibrations. Data is only presented up to 1100 cm^{-1} due to degradation of peak resolution at higher frequencies as a result of increasing contributions from combination and overtone vibrations. The vibrational analysis presented in Table 1 shows the perylene vibrational motion dominates the INS spectrum of the complex. This is to be suspected as TCNE has no protons. Several TCNE modes do appear in the INS spectrum, however, and these must contain a significant component of hydrogen motion from the perylene. A comparison between the INS frequencies of the TCNE–perylene complex and the neat perylene [19] reveals the effect of the electron donor–acceptor interaction on the vibrational modes. In several instances, the out-of-plane vibrations deviate considerably with an average difference of 15 cm^{-1}. Vibrational frequency differences of this magnitude for the out-of-plane motion may be rationalized on the basis of comparison of the structure of the complex relative to neat perylene. The perylene molecules in the complex behave more freely because they are interspersed with TCNE units and have more room to vibrate out-of-plane, resulting in slightly higher frequency values.

The experimental INS and vibrational frequencies calculated with the isolated complex B3LYP/6-31G** method and the solid-state PW91 and BLYP/dnd methods are shown in Table 1. The majority of the calculated frequencies deviate from the experimental INS frequencies by less than 10 cm^{-1} for all three methods. The RMS deviation from the experimental frequencies obtained from the FANS instrument is 5.45 cm^{-1} for the scaled B3LYP/6-31G** calculations. The RMS values of the FANS data decrease slightly with the solid-state periodic methods to 3.21 cm^{-1} (PW91) and 3.76 cm^{-1} (BLYP/dnd). The RMS values for the TOSCA experimental frequencies are, at 6.58 cm^{-1} (B3LYP/6-31G**), 4.57 cm^{-1} (PW91), and 5.20 cm^{-1} (BLYP/dnd), slightly larger than the FANS RMS values. These slight deviations in the RMS values and experimental frequencies obtained from the two instruments can be attributed to differences in the instrumental resolution.

The six intermolecular vibrations of the complex are predicted to appear below 110 cm^{-1} by all three methods. Fig. 2a, which presents a comparison of the experimental and calculated spectra up to 600 cm^{-1}, shows that five of the six modes appear in both spectra. The vibrational mode observed at 42 cm^{-1} in the TOSCA spectrum, which is near the limit of the spectral range of the FANS instrument, can be attributed to the twisting mode at 43 cm^{-1} (B3LYP/6-31G**), 40 cm^{-1} (PW91) or 35 cm^{-1} (BLYP/dnd). Two TCNE–perylene intermolecular bond stretching modes are calculated at 55 cm^{-1} (B3LYP/6-31G**), 59 cm^{-1} (PW91), and 63 cm^{-1} (BLYP/dnd) and 73 cm^{-1} (B3LYP/6-31G**), 70 cm^{-1} (PW91) and 75 cm^{-1} (BLYP/dnd) can be paired with the experimental transitions at 59 and 69 cm^{-1} of the TOSCA spectrum (56 and 70 cm^{-1}, FANS spectrum). The transition observed in the experimental spectra at 84 cm^{-1} (TOSCA) and 83 cm^{-1} (FANS) can be assigned as the TCNE–perylene tilting mode calculated at 85 cm^{-1} (B3LYP/6-31G**), 83 cm^{-1} (PW91) and 92 cm^{-1} (BLYP/dnd). A sliding mode of the TCNE—perylene complex is calculated at 104 cm^{-1} (B3LYP/6-31G**), 106 cm^{-1} (PW91), and 110 cm^{-1} (BLYP/dnd) can be assigned to the experimental peaks at 106 cm^{-1} (TOSCA) and 107 cm^{-1} (FANS). The sixth intermolecular mode is experimentally observed at 30 cm^{-1} in only the TOSCA spectrum and can be assigned to as a sliding motion of the TCNE–perylene components, which is calculated at 26 cm^{-1} (B3LYP/6-31G**), 23 cm^{-1} (PW91) and 26 cm^{-1} (BLYP/dnd).

The vibrational frequencies of the modes below 200 cm^{-1} are reproduced with reasonable accuracy with all the three methods. The best intensity prediction is given by the BLYP/dnd. It is not surprising to note the slight errors in the intensities predicted by the B3LYP/6-31G** method, as this is commonly a region dominated by phonons. The poor intensity agreement of the PW91 spectrum can probably be attributed to the small supercell used for the simulations. It is likely that the use of a larger cell would improve the agreement.

The spectral region between 200 and 1100 cm^{-1} is characterized by several intense vibrations and is shown in Fig. 2a and b. The majority of these vibrational peaks are well represented both in frequency and intensity by all three theoretical methods, as is shown in Table 1. This result is not surprising as vibrations above 300 cm^{-1} typically are less influenced by dispersion forces. Over this vibrational range, Fig. 2 and Table 1 show the PW91 method gives vibrational frequencies and intensities which are in better agreement with the experimental values compared to the B3LYP/6-31G** and BLYP/dnd calculations, which give slightly red-shifted values.

Five out-of-plane C–C–C bending vibrations are observed in the frequency range of 200–700 cm^{-1}. These vibrations are all adequately described by the calculations and suggest that the intermolecular spacings of the optimized geometries are comparable to the crystal spacings. If the calculated intermolecular spacing were substantially different from experiment, one would expect significant differences in vibrational intensities and frequencies. The correctness of the calculated intermolecular separation distances are also indicated by the close agreement of the out-of-plane C–C–H bending vibrations between 650 and 1100 cm^{-1}. For these

Table 1
The assignment of the vibrational modes as observed in the experimental and calculated inelastic neutron scattering spectra of TCNE–perylene and perylene

TOSCA–perylene [19]	TOSCA-complex	FANS-complex	B3LYP/6-31G**	PW91	BLYP/dnd	Molecular motion
	30		26	23	26	TCNE–perylene sliding
	42	43	43	40	35	TCNE–perylene twisting
	59	56	55	59	63	TCNE–perylene stretching
	69	70	73	70	75	TCNE–perylene stretching
	84	83	85	83	92	TCNE–perylene tilting
	106	107	104	106	110	TCNE–perylene sliding
128	131	129	136	127	130	OP C–C–C bend (P)
	144	144	150	149	150	C–CN IP torsion (T)
	147	155	156	156	160	TCNE scissor mode (T)
157	NR	187	182	180	195	OP C–C–C bend (P)
192	196	191	190	191	194	OP C–C–C bend (P)
221	NR	201	199	204	203	OP C–C–C bend (P)
	226	224	211	227	225	TCNE skeletal def. IP (T)
235	230	229	231	234	229	OP C–C–C bend (P)
	NR	243	240	240	235	C–CN bend (T)
258	248	253	251	254	256	OP C–C–C bend (P)
	282	279	278	278	280	nitrile stretch IP (T)
303	293	295	301	297	303	OP C–C–C bend (P)
357	349	350	352	351	349	IP C–C–C bend (P)
368	363	363	365	364	361	IP C–C–C bend (P)
421	416	420	422	424	415	OP C–C–C bend (P)
434	426	425	431	434	430	IP C–C–C bend (P)
454	456	458	458	458	457	OP C–C–C bend (P)
467	470	470	468	470	466	IP C–C–C bend (P)
NR	487	487	485	486	482	OP C–C–C bend (P)
522	520	516	522	518	519	OP C–C–C bend (P)
530	525	527	528	524	523	IP C–C–C bend (P)
554	544	543	545	547	539	IP C–C stretch (T)
NR	566	568	559	567	570	C–C–CN bend IP (T)
585	586	583	583	581	580	IP C–C–C bend (P)
	592	594	590	594	595	C–C–CN bend OP (T)
612 (sh)	607	607	600	604	605	OP C–C–C bend (P)
631	622	622	625	623	623	OP C–C–C bend (P)
653	650	648	654	645	653	OP C–C–C bend (P)
NR	656	660	661	659	660	OP C–C–C–bend (P)
NR	670	667	663	666	667	OP C–C–H bend (P)
694	NR	679	686	681	682	OP C–C–C bend (P)
721	708	704	704	704	708	OP C–C–H bend (P)
NR	719	718	720	723	719	IP C–C–C bend (P)
NR	726	725	723	726	725	IP C–C–C bend (P)
769	741	743	764	749	746	OP C–C–H bend (P)
NR	774	775	776	776	776	IP C–C–C bend (P)
797	790	784	782	791	782	OP C–C–H bend (P)
821	810	805	801	802	802	OP C–C–H bend (P)
830	818	818	818	819	817	OP C–C–H bend (P)
855	830	829	824	831	833	OP C–C–H bend (P)
863	847	839	841	843	840	OP C–C–H bend (P)
NR	NR	865	859	867	868	IP C–C stretch (T)
899	877	876	874	881	878	OP C–C–H bend (P)
916	908	904	905	907	910	OP C–C–H bend (P)
935	941	939	926	940	935	OP C–C–H bend (P)
954	NR	951	964	954	952	OP C–C–H bend (P)
978	985	983	990	980	986	IP C–C stretch (T)
NR	1004	NR	997	1000	1004	C–C stretch (T)
NR	NR	1015	1010	1011	1013	C–C–C stretch (T)
NR	1034	1036	1036	1037	1033	IP C–C stretch (T)
NR	1052	1057	1057	1057	1056	IP C–C stretch (T)
NR	1066	1071	1075	1068	1070	IP C–C stretch (T)
1102	1087	1093	1090	1100	1093	IP C–C stretch (P)

All values are reported in cm^{-1}. Tentative assignments of molecular motions are also provided. The notation for the molecular motion is as follows: (T) TCNE mode; (P) perylene mode; OP, out-of-plane; IP, in-plane; NR indicates peak was not resolvable.

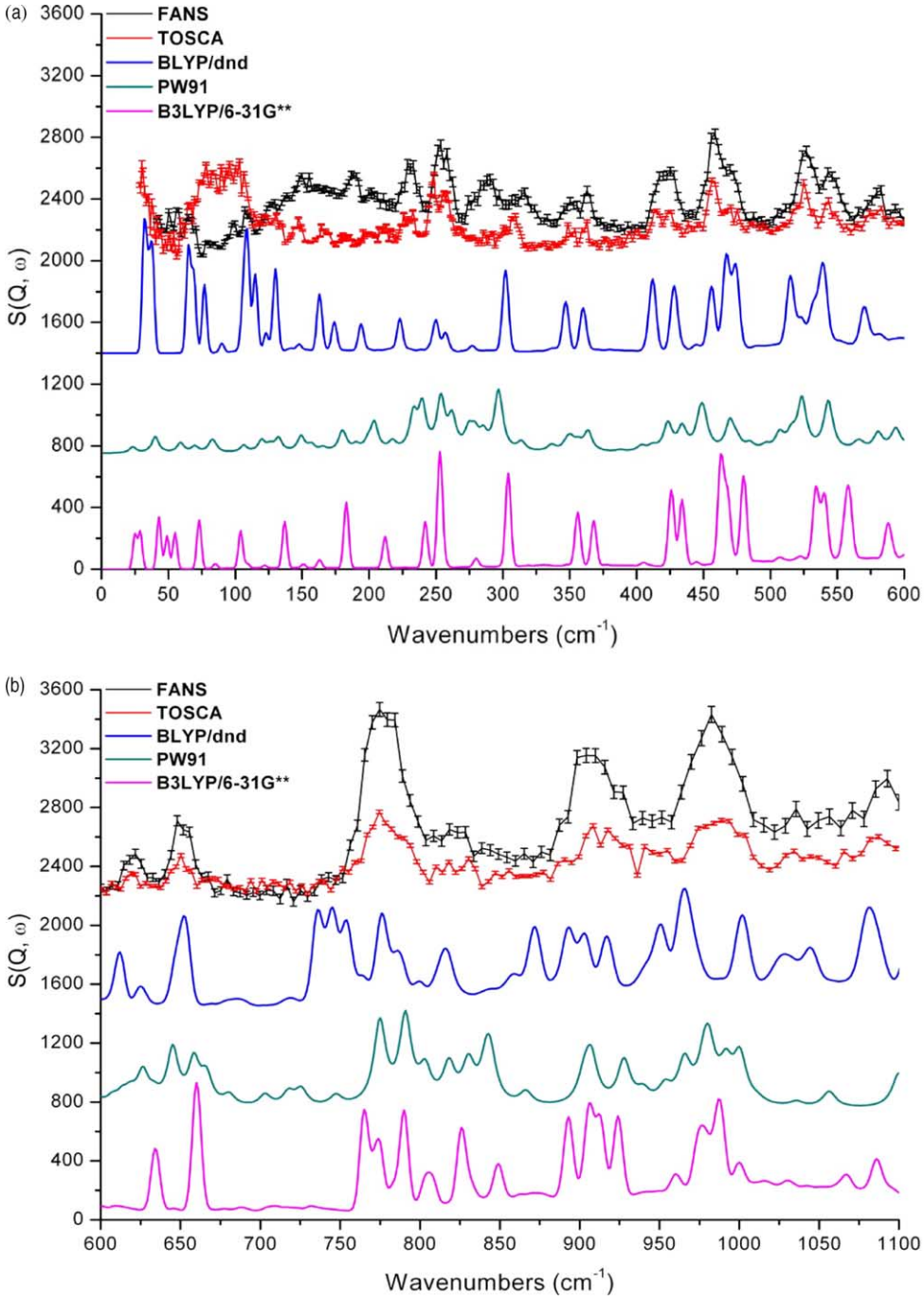

Fig. 2. A comparison of the experimental INS spectrum of TCNE–perylene and spectra constructed from density functional theory using the isolated molecule B3LYP/6-31G** method and the solid-state BLYP/dnd and PW91 methods are shown from (a) 0–600 cm^{-1} and (b) 600–1100 cm^{-1}. Each spectra is off-set by a constant for clarity.

vibrations, however, the PW91 calculations seem to give slightly better intensity agreement than the other two methods.

4. Conclusions

The present study between the experimental and theoretical inelastic neutron scattering vibrations clearly demonstrates the power of a combined experimental/theoretical approach when studying intermolecular interactions of EDA complexes, such as TCNE–perylene. Both the PW91 and BLYP/dnd solid-state methods predict vibrational frequencies that agree well with the INS measured frequencies over the entire spectral range considered. The PW91 method was found to be slightly superior to the BLYP/dnd and B3LYP/6-31G** methods, which, in general, gave slightly red-shifted vibrational frequencies. In general, all three calculations yielded reasonably accurate intensities above 200 cm^{-1}. Below 200 cm^{-1}, the intensities of the PW91 calculations did not compare well with experimental data due to the small size of our supercell.

The accuracy of the calculations when compared to experiment yields two important conclusions and considerations for future work on this complex and other EDA complexes. First, in order to accurately model the vibrational intensities of the low frequency spectrum, larger supercells than the one employed here must be used. In addition, an attempt must be made to model the interactions between the unit cells in order to reflect a continuous unit of alternating donor and acceptor molecules. Second, our calculations show that solid-state calculations are not necessary, at least in the case of the TCNE–perylene complex, to obtain a reliable vibrational fequency representation. This may be unique to the TCNE–perylene complex, but a systematic study of several EDA complexes is currently underway to test this idea.

Acknowledgements

The NIST Center for Neutron Research is acknowledged for providing neutron beam access on the FANS instrument. The ISIS facility of the Rutherford Appleton Laboratory is thanked for access to the TOSCA instrument. The Army Research Laboratory Major Shared Resource Center is thanked for access and support of the VASP program. An NRC Fellowship with the Army Research Laboratory partially supported J.C. during the course of this research.

References

[1] J. Singleton, J. Solid-State Chem. 168 (2002) 675.
[2] J.A. Ciezak, B.S. Hudson, J. Mol. Struct. TheoChem. 755 (2005) 195.
[3] I. Ikemoto, K. Yakushi, H. Kuroda, Acta Crystallogr. B26 (1970) 800.
[4] R.S. Mulliken, J. Am. Chem. Soc. 74 (1952) 811.
[5] H. Kuroda, I. Ikemoto, H. Akamatu, Bull. Chem. Soc. Jpn 39 (1966) 547.
[6] R.M. Williams, S.C. Wallwork, Acta Crystallogr. 22 (1967) 899.
[7] T. Gotoh, T. Kondoh, K. Egawa, K. Kubodera, J. Opt. Soc. Am. B6 (1989) 703.
[8] B.S. Hudson, J. Phys. Chem. A105 (2001) 3949.
[9] M. Montejo, A. Navarro, G.J. Kearley, J. Vazquez, J.J. Lopez-Gonzalez, J. Am. Chem. Soc. 126 (2004) 15087.
[10] J.C. Li, A.I. Kolesnikov, J. Mol. Liq. 100 (2002) 1.
[11] M. Plazanet, M.R. Johnson, J.D. Gale, T. Yildrim, G.J. Kearley, M.T. Fernadez-Diaz, D. Sanchez-Portal, E. Artacho, J.M. Soler, P. Ordejon, A. Garcia, H.P. Trommsdorff, Chem. Phys. 261 (2000) 189.
[12] B. Paci, M.S. Deleuze, R. Caciuffo, A. Arduini, F. Zerbetto, Mol. Phys. 98 (2000) 567.
[13] W. Sawka-Dobrowolska, G. Bator, L. Sobczyk, A. Pawkukojc, H. Ptasiwicz-Bak, H. Rundlof, J. Krawczyk, M. Nowina-Konopka, P. Jagielski, J.A. Janik, M. Prager, O. Steinsvoll, E. Grech, J. Nowicka-Scheibe, J. Chem. Phys. 123 (2005) 124305.
[14] T.J. Udovic, D.A. Neumann, J. Leão, C.M. Brown, Nucl. Instr. Meth. A517 (2004) 189.
[15] Certain commercial programs, instruments, and materials are identified in this paper to foster understanding. Such identification does not imply recommendation or endorsement by the National Institute of Standards and Technology, nor does it imply that the materials or equipment identified are necessarily the best available for the purpose.
[16] S.F. Parker, C.J. Carlile, T. Pike, J. Tomkinson, R.J. Newport, C. Andreani, F.P. Ricci, F. Sachetti, M. Zoppi, Physica B 241–242 (1998) 154.
[17] Z.A. Bowden, M. Celli, F. Cilloco, D. Colognesi, R.J. Newport, S.F. Parker, R.P. Ricci, V. Rossi-Albertini, F. Sacchetti, J. Tomkinson, M. Zoppi, Physica B 276–278 (2000) 98.
[18] M. Celli, F. Cilloco, D. Colognesi, R.J. Newport, S.F. Parker, V. Rossi-Albertini, F. Sacchetti, J. Tomkinson, M. Zoppi, Notiziaro Neutrone e Luce di Synchrotrone 6 (2001).
[19] F. Filaux, Fuel 74 (1995) 865.
[20] http://www.ncnr.nist.gov/dave
[21] A.D. Becke, J. Chem. Phys. 88 (1988) 2547.
[22] B. Delley, J. Chem. Phys. 113 (2003) 7756.
[23] B. Delley, J. Chem. Phys. 92 (1992) 508.
[24] J.P. Perdew, in: P. Ziesche, H. Eschrig (Eds.), Electronic Structures of Solids '91, Akademie-Verlag, Berlin, 1991.
[25] G. Kresse, J. Furthmuller, Vienna Ab-Initio Simulation Package (VASP); VASP Group, Institut fur Materialphysik, Universitat Wein, Sensengasse 8, A-1130 Wein, Vienna, Austria, 2003.
[26] D. Vanderbuilt, Phys. Rev. B41 (1990) 7892.
[27] A.D. Becke, J. Chem. Phys. 98 (1993) 5648.
[28] M.J. Frisch, et al. GAUSSIAN 98 (Revision A7), Gaussian, Inc., Pittsburgh, PA, 2001.
[29] A.J. Ramirez-Cuesta, Comp. Phys. Comm. 157 (2004) 226.